Lattice dynamics of perovskite $Pb_xCa_{1-x}TiO_3$

Shou-Yi Kuo
Precision Instrument Development Center, National Science Council, Hsinchu, Taiwan 30050, Republic of China

Chung-Ting Li and Wen-Feng Hsieh*
Institute of Electro-Optical Engineering, National Chiao Tung University, Hsinchu, Taiwan 30050, Republic of China
(Received 5 October 2003; revised manuscript received 20 January 2004; published 25 May 2004)

Investigation of the structural and vibrational properties of the $Pb_xCa_{1-x}TiO_3$ (PCT) system exhibits two phase transitions in the range of $x=0-1$ by using x-ray powder diffraction and Raman spectroscopy. The first transition occurring at $x\sim0.65$ corresponds to the tetragonal-to-cubic phase and the second one occurs near $x=0.35$ is attributed to the orthorhombic-to-cubic phase. The absence of the intermediate tetragonal phase between orthorhombic and cubic phases ($0<x<0.35$) may be mostly attributed to the very restricted region in the PCT system. In addition, a decreasing giant LO-TO splitting behavior similar to that exhibited in $Pb_xSr_{1-x}TiO_3$ system for lower Pb concentration was also observed, which has been attributed to the highly Pb-O covalent bonding to reduce the long-range Coulomb interaction. Comparison of the change of line shapes of $A_1(1TO)$ mode among three $PbTiO_3$-based perovskites indicates that the anharmonicity will become more conspicuous due to the larger high-order potential terms of Ba^{2+} and Ca^{2+} substitution than Sr^{2+} substitution for Pb^{2+}.

DOI: 10.1103/PhysRevB.69.184104 PACS number(s): 61.10.Nz, 63.20.Dj, 63.20.Ry

I. INTRODUCTION

In the past, the ABO_3 perovskite-type oxides have been extensively studied mainly not only for their technical applications but also for fundamental research. Their simple crystal structure, and the variety of structural phase transitions which they display, make them suitable for experimental study and for testing theoretical models.

There is great progress in understanding the lattice dynamics, dielectric properties, and phase-transition phenomena of oxide perovskite using first-principles calculations during recent years.[1–4] The relatively simple sequences of phase transitions in $PbTiO_3$, $BaTiO_3$, $KNbO_3$, and $SrTiO_3$ have been reproduced using Monte Carlo simulations, whereas the complex sequences in $CaTiO_3$ (CTO) have not yet been successfully reproduced.[5]

The prototype perovskite structure is cubic ($Pm3m, O_h^1$), but the structure of CTO at room temperature is orthorhombic with a quadrupled unit cell ($Pbnm, D_{2h}^{16}$).[6–8] Although the deviations from the cubic are small, the crystal keeps its pseudocubic character with cell parameters down to low temperature. The first evidence of a high-temperature phase transition was found in the 1940s,[9] but the problem of high-temperature structures has recently been the subject of intense study.[10–13] Earlier studies on phase transition of pure CTO were investigated by high-temperature x-ray diffraction (XRD), which shows the orthorhombic distortion of CTO decreases as the temperature increases, but failed to reach high enough temperature to directly observe a transition to higher symmetry.[14,15] Neutron diffraction was employed by Vogt *et al.*[10] to find a direct transformation from orthorhombic to cubic, without intermediate tetragonal phase. More recently, Redfern,[11] by *in situ* x-ray diffraction, presented experimental evidence for the existence of an intermediate tetragonal phase between orthorhombic and cubic structures. Matsui *et al.*[12] have also found the presence of an intermediate phase by high-temperature x-ray diffraction. Based on the high-temperature neutron-diffraction measurements, detailed structural transitions have been reported by Kennedy *et al.*[13] It is now clear that CTO undergoes at least two, but probably three, phase transitions at high temperature.

In technical application among various $PbTiO_3$-based ferroelectrics, $Pb_xCa_{1-x}TiO_3$ (PCT) is a promising material for practical use in piezoelectric transducers for ultrasonic nondestructive control devices and imaging applications due to the unusually large anisotropic piezoelectric response.[16–19] Although there have been a number of studies on the Ca-modified $PbTiO_3$ ceramics, most of them focused on the electric properties, it still lacks for detailed analysis on lattice dynamics. It has been recognized that the lattice-dynamical properties should play a key role on ferroelectricity and related properties.[20] Moreover, our earlier studies on $Ba_xSr_{1-x}TiO_3$ (BST) and $Pb_xSr_{1-x}TiO_3$ (PST) systems have shown that both similar systems exhibit anomalous discrepancy in lattice dynamics.[21] Therefore, further systematic study is needed to clarify lattice dynamics of the PCT system.

Foster *et al.*[22,23] have first reported the anharmonicity for the $A_1(1TO)$ mode of $PbTiO_3$ consisting of four subpeaks, and similar behavior were also found in Nd-modified lead titanate and lead zirconate titanate ceramics.[24,25] They advocated that the $A_1(1TO)$ mode has a double-well potential in the ferroelectric state and the anharmonicity of the double-well potential is the origin of the observed subpeak structure. In contrast to the earlier studies of slight *A* and *B* cation substitutions,[24,25] here, we discuss the effect of isovalent *A* cation substitutions of $PbTiO_3$. From XRD measurements, the variations of lattice constants were calculated for the polycrystalline $Pb_xCa_{1-x}TiO_3$ powders with *x* varying from 0 to 1. In addition, Raman spectroscopy provides an *in situ* observation of structural changes. The phase transitions differing from $CaTiO_3$ and $Ca_xSr_{1-x}TiO_3$ systems are charac-

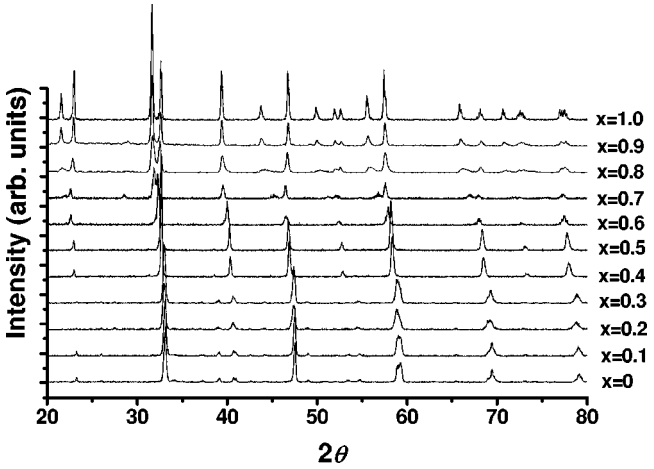

FIG. 1. Powder XRD patterns of $Pb_xCa_{1-x}TiO_3$ samples with various x values.

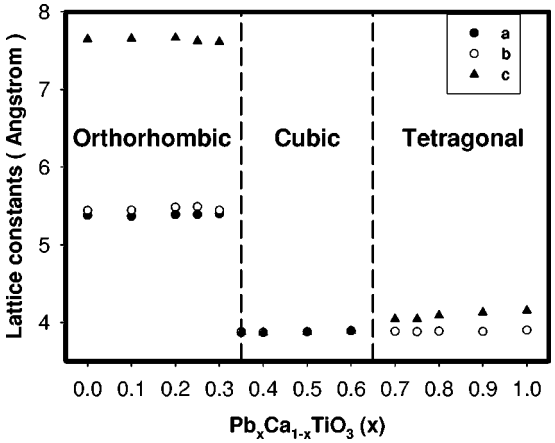

FIG. 2. The lattice constants a, b, and c of $Pb_xCa_{1-x}TiO_3$ after Rietveld refinement. The figures indicate the material is tetragonal for $x>0.65$, cubic in the region $0.35<x<1.65$ and orthorhombic while $x<0.35$.

terized. Detailed analyses on lattice dynamics are discussed by applying the anharmonic approximation.

II. EXPERIMENT

Sol-gel technique was employed in our experiments for preparing $Pb_xCa_{1-x}TiO_3$ polycrystalline powders to yield samples with high composition accuracy and homogeneity. Lead acetate and calcium acetate dissolved in dehydrated acetic acid and Ti-isopropoxide were used as the raw materials. Detailed procedure was similar to that described elsewhere.[21,26] Ceramic pellets of about 10 mm diameter and 1–2 mm thickness were obtained by sintering at 1300 °C for 3 h. In contrast to the conventional solid-state reaction method, the atom arrangement using sol-gel technique was determined under gelation at lower temperature. Moreover, the sintering temperature is far below the melting point of PCT, thus it provides insufficient energy to cause extra atom rearrangement to result in lattice relaxation.

X-ray powder diffraction patterns were obtained using a SHIMADZA XD-5 diffractometer and monochromated high intensity Cu-$k\alpha$ line of 1.5405 Å over the range $20°<2\theta<80°$. The XRD patterns were then Gaussian fitted to get the diffraction peaks and widths as described elsewhere.[26] Raman spectra were excited using the 488 nm line of Ar^+ laser and analyzed using a SPEX 1877C triple spectrograph equipped with a cooled charg-coupled device. In addition, the experimental results of PCT are compared with those of PST and BST systems to account for the influence of cation substitution.

III. RESULTS AND DISCUSSION

Shown in Fig. 1 are the XRD patterns of the $Pb_xCa_{1-x}TiO_3$ samples prepared by the aforementioned sol-gel processes with various x. The patterns were collected at room temperature and the structural refinements were then undertaken with Rietveld program. The lattice parameters and the denoted structural phases after the best fitted refinement procedure are shown in Fig. 2. Preliminary analysis of XRD patterns indicated that the material is tetragonal for $x>0.65$, cubic in the region $0.35<x<0.65$, and orthorhombic while $x<0.35$.

In contrast with earlier studies of phase transitions on $CaTiO_3$ and the related materials, it can be seen that no intermediate phases were resolved in our analysis. From the detailed Rietveld analyses of CTO powder neutron-diffraction data acquired at high temperature, Kennedy *et al.*[13] have observed an intermediate tetragonal structure forming near 1500 K and the primitive cubic structure above 1580 K. The existence of intermediate tetragonal phase was found in several researches on $Ca_xSr_{1-x}TiO_3$ as well.[27–29] It has been well known that CTO belongs to orthorhombic phase at room temperature (~300 K). According to the structural phase transitions on CTO by Kennedy *et al.*,[13] the region of tetragonal-to-cubic transition only occupied 6% of the orthorhombic-to-cubic transition while the temperatures were increased from room temperature to forming cubic phase. From our XRD analyses, it reveals that PCT system exhibits different structural transitions from pure $CaTiO_3$ and $Ca_xSr_{1-x}TiO_3$ systems. More data taken by finer stoichiometry steps in the immediate vicinity of the orthorhombic-to-cubic transition did not show the intermediate phase either. Hence, the disappearance of the tetragonal phase between orthorhombic and cubic phases in the PCT system may be attributed to the limited stoichiometry region.

The Raman spectra of $Pb_xCa_{1-x}TiO_3$ polycrystalline powders taken at room temperature are plotted in Fig. 3 for various x values. As x decreases from 1 to 0.65, the phonon modes have remarkable changes in their line shapes. Also, these peaks not only show evidently frequency shift but also weakens or disappears when $x<0.65$. The observed Raman spectra became noisy when $x<0.65$. It is interesting to note that $Pb_xCa_{1-x}TiO_3$ undergoes a phase transition from ferroelectric to paraelectric phase when $x\sim0.65$. Besides, the Raman spectrum of our $PbTiO_3$ sample coincides with the earlier literature, and the phonon modes given in Fig. 4 are characterized according to those of Foster *et al.*[22,23] In the paraelectric phase, $PbTiO_3$ is cubic and belongs to the O_{1h}

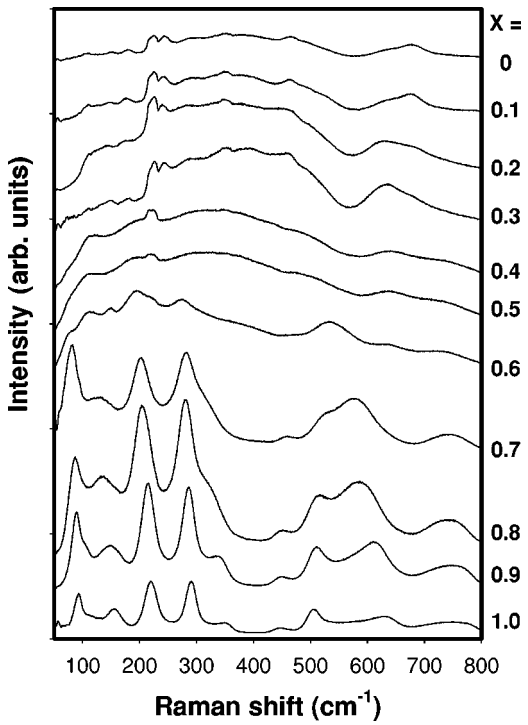

FIG. 3. Room temperature Raman spectra of $Pb_xCa_{1-x}TiO_3$ for x between 0 and 1.0.

$(Fm3m)$ space group with one formula unit per unit cell. There are 12 optical phonon modes at the Brillouin zone center, which transform as $3T_{1u}+T_{2u}$ in the irreducible representation. The T_{1u} modes are infrared active and the T_{2u} mode is silent, neither infrared nor Raman active. Hence, the broadened spectra observed in the paraelectric phase indicate

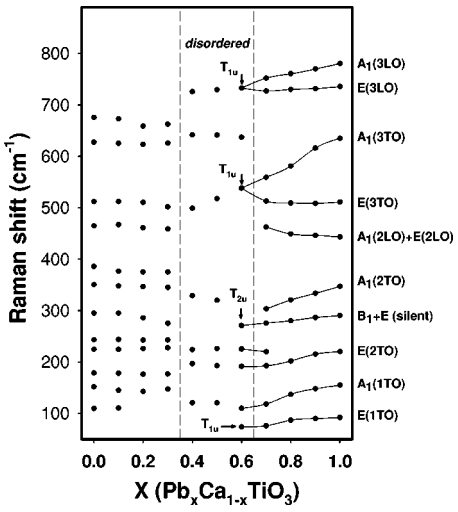

FIG. 4. The x dependent phonon modes of the polycrystalline $Pb_xCa_{1-x}TiO_3$. The dotted symbols represent as-read peaks and fitting results of $E(3LO)$ and $A1(3LO)$ modes, respectively. The symmetry assignments of phonon modes are labeled along the principal axes while PCT are in tetragonal phase ($x>0.65$), and the observed peaks in the cubic phase, $0.35<x<0.65$, were labeled as "*disordered.*" The solid lines are eye-guided to view the tendency of phonon modes as lowering x from 1.0 to 0.6.

that the Raman selection rule is relaxed ascribed to the disorder in unit cells of the polycrystalline. The peaks observed in the cubic phase were labeled as "disordered" in Fig. 4. Then, through the displacive ferroelectric phase transition, $PbTiO_3$ becomes tetragonal with the space group, $C_{4v}^1(P4mm)$. Modes in each of the three T_{1u} in the paraelectric phase split into two modes transforming as A_1+E, and the T_{2u} mode splits into two modes transforming as B_1+E. All modes are both Raman and infrared active. Therefore, the optical phonon modes of the ferroelectric $PbTiO_3$ consist of $3A_1+B_1+4E$ modes as shown in Fig. 4. However, the split of T_{2u} into B_1+E has not been observed, and the B_1+E modes were classified as "silent" modes. On the other side, the Raman spectrum of the other end member, $CaTiO_3$, are observed in accordance with the results in Refs. 30 and 31. A number of studies have reported infrared and Raman spectra for $CaTiO_3$.[32–36] Actually, 117 vibrational modes $(\Gamma_{vibr}=7A_g+8A_u+7B_{1g}+8B_{1u}+5B_{2g}+10B_{2u}+5B_{3g}+10B_{3u})$ are expected for orthorhombic $CaTiO_3$, but most of these modes cannot be detected because of overlapping of bands and their low polarizabilities. Therefore, interpretation of the data is difficult.

From the Raman spectra displayed in Fig. 3, the Pb concentration dependence of the peak positions is clearly shown. Also, the frequencies of the phonon modes in PCT system are plot in Fig. 4, and the symmetry assignments established from the data are labeled along the principal axes. The complete Pb concentration dependence shown in Fig. 4 will allow us to clarify the structural variation via frequency degeneracy. Moreover, it can be seen clearly from Fig. 3 that the Raman spectra change gradually so that we can conclude that there are at least two structural transformations that occurred in the PCT system. First, a tetragonal to cubic phase transition was found at composition $x\sim0.65$ of the PCT powders, which agrees with the XRD analyses. It has been well known that $PbTiO_3$ belongs to tetragonal phase at room temperature. The addition of Ca is used to decrease the tetragonality and transition temperature. It has become customary to classify ferroelectrics by the properties of the soft optical modes. According to the lattice-dynamical theory, of particular, vibrational soft modes are expected to be associated with the phase transitions. The $A_1(1TO)$ mode is of special interest, since it is the softest mode together with the $E(1TO)$ mode. From Fig. 4, these lowest TO phonon modes gradually soften and broaden their linewidth with increasing Ca content, which reflects that the ferroelectric phase becomes unstable. The mode softening becomes unapparent as the Ca content reaches 0.4 $(x=0.6)$, which suggests that the cubic phase has been formed in the $Pb_xCa_{1-x}TiO_3$ system.

In addition to mode softening, the $A_1(1TO)$ mode exhibits an anomalous line shape in the range $0.7<x<1$. For uniaxial crystal, e.g., $PbTiO_3$, asymmetric line shape of the $A_1(1TO)$ modes may mainly originate from oblique phonons and anharmonic nature of the lattice. It was found by Foster *et al.*[23] that the anomalous line shape of the A_1 (1TO) Raman peak in $PbTiO_3$ single crystal is not a smooth function but appears to be a superposition of four subpeaks at room temperature. Although it is impossible to ignore the influences of

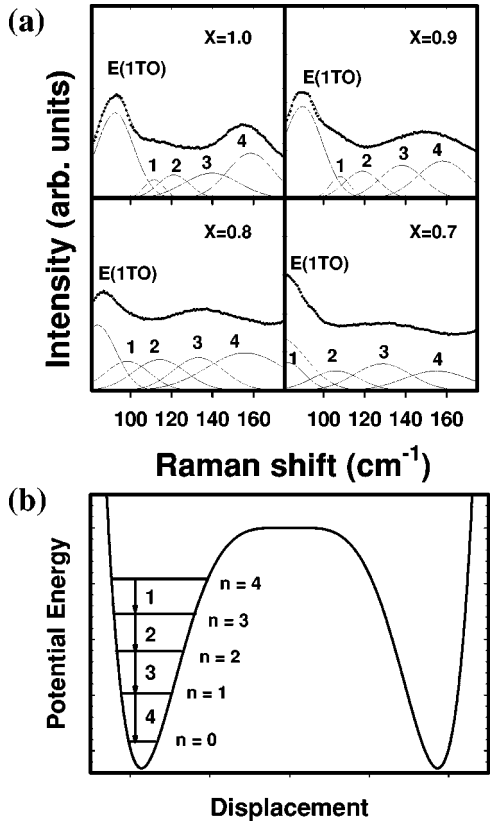

FIG. 5. (a) Raman spectra measured from $Pb_xCa_{1-x}TiO_3$ samples with $x=1.0$, 0.9, 0.8, and 0.7 together with a peak fitting for all four spectra. (b) Schematic representation of the double-well potential of $PbTiO_3$ illustrating the anharmonic nature of the potential of the $A_1(1TO)$ phonon, where n denote the quantum number.

oblique phonons, multiple subpeaks of the $A_1(1TO)$ phonon were observed in the Nd-modified lead zirconate titanate and lead titanate ceramics and give qualitative agreement to the anharmonic potential model as well. Referring to those literatures, our Raman results do reveal a subpeak structure of tetragonal $A_1(1TO)$-mode frequencies and it is believed that the anharmonic model can be used to be an auxiliary indicator on the anharmonicity of $A_1(1TO)$ mode.

By including E(1TO) and using anharmonic model to decompose the $E(1TO)$ and $A_1(1TO)$ modes, we show in Fig. 5(a) the fitting results of the $E(1TO)$ and $A_1(1TO)$ modes of $Pb_xCa_{1-x}TiO_3$ at $x=1$, 0.9, 0.8, and 0.7. The four subpeaks of $A_1(1TO)$ mode labeled 1, 2, 3, and 4, respectively, correspond to the transitions from $n=0$ to $n=1$, $n=1$ to $n=2$, $n=2$ to $n=3$, and $n=3$ to $n=4$ of the vibrational quantum states. We illustrate these transitions in Fig. 5(b), where the energy levels shown in one side of the double well describe the possible phonon states associated with the $A_1(1TO)$ mode.

Figure 6 shows the Pb concentration dependence of subpeak frequencies of the $A_1(1TO)$ mode. It is obvious that all four subpeaks evidently show a softening behavior with decreasing Pb concentration although the subpeak 4 changes less than other subpeaks. Earlier study on x-ray near edge structure (XANES) spectra has revealed that the Ca substitution for Pb decreases Pb-O and Ti-O hybridization,[37] which

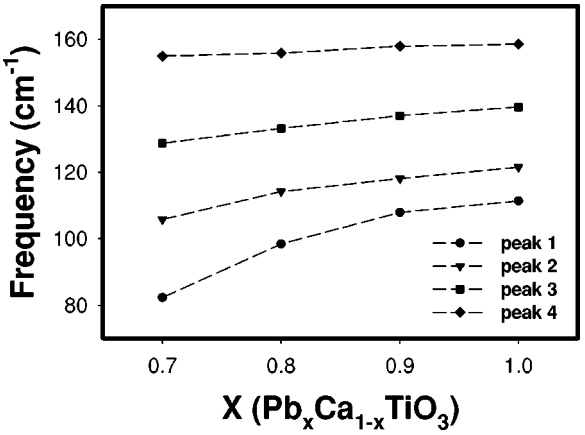

FIG. 6. The Pb concentration dependence of the subpeak frequencies of the $A_1(1TO)$ mode of the $Pb_xCa_{1-x}TiO_3$ samples, showing the softening behavior and splitting tendency between sequential subpeaks as x decreases from 1.0 to 0.7.

implicitly indicates the lowering of bond strength and thus the softening of phonon frequency. The softening behavior of $A_1(1TO)$ mode has also been observed in undoped $PbTiO_3$ single crystal with increasing measurement temperature.[22,23] The frequency of each subpeak is the transition energy between two corresponding states. Therefore, the spacing between subpeak frequencies is the difference of their transition energies. In case of harmonic oscillator, the energy difference is zero. Thus, the nonzero spacing between subpeak frequencies as indicated in Fig. 6 seems to be caused by the anharmonicity of lattice potential. From the above-mentioned description, we can conclude that the change of the broad $A_1(1TO)$ feature with decreasing x might be related to the softening and anharmonic effect of the $A_1(1TO)$ mode. In view of the Landau theory, the potential energy can be expressed as[38]

$$\Phi(q')=\frac{k}{2}q'^2+\frac{\xi}{4}q'^4+\frac{\zeta}{6}q'^6, \tag{1}$$

where q' is the normal mode coordinate, and k, ξ, and ζ are the potential parameters, respectively. This potential energy has been schematically shown in Fig. 5(b). It should be noted that the negative coefficient ξ in the q'^4 term signifies the fact that $PbTiO_3$ has a first-order transition character. After a tedious transformation procedure of moving the origin of $\Phi(q')$ to one of the two minima in the double-well potential, one can obtain the Hamiltonian operator,[39,40]

$$H=H_0+H', \tag{2}$$

where H_0 is the Hamiltonian of harmonic oscillator, and H' is the anharmonic term. To simplify the calculation, we have taken up to the quartic term to obtain $H'=aq+cq^3+dq^4$, where a, c, and d are variables depending on the parameters k, ξ, and ζ. According to the second-order perturbation theory, the difference of the subpeak frequencies between two adjacent vibrational transitions is given by[39,40]

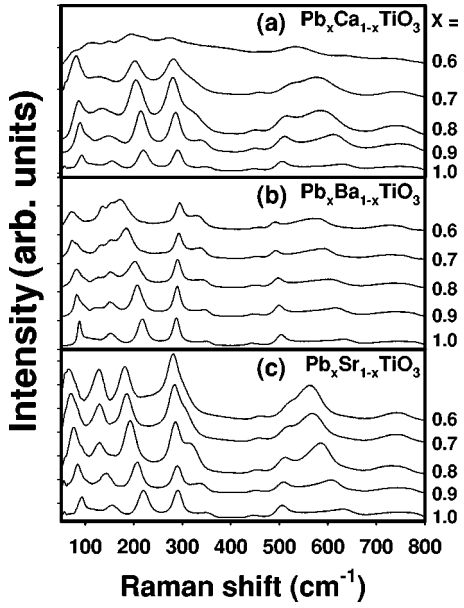

FIG. 7. Room temperature Raman spectra for (a) $Pb_xCa_{1-x}TiO_3$, (b) $Pb_xBa_{1-x}TiO_3$, and (c) $Pb_xSr_{1-x}TiO_3$ samples with x between 1.0 and 0.6.

$$\hbar\omega_n - \hbar\omega_{n+1} = \frac{\hbar^2}{2m^2\omega_0^2}\left(15\frac{c^2}{m\omega_0^2} - 6d\right), \tag{3}$$

where $\hbar\omega_n$ is the net difference in the energy eigenvalues between the nth and the $(n-1)$th vibrational state and m the reduced mass. The addition of Ca content in the PCT system lowers the Curie temperature to cause phonon softening. Among the parameters appearing in Eq. (3), ω_0 is expected to have the most prominent Pb concentration dependence to lead to the increase of the spacing between the subpeak frequencies while lowering tetragonality toward cubic phase. In Fig. 6, the spacing shows splitting behavior as expected, which implies the validity of the anharmonic model even though the spacings are unequal due to higher-order perturbation corrections.[22,23]

In order to investigate the influence on lattice dynamics of various A cation substitutions of $PbTiO_3$, Raman spectra of $Pb_xBa_{1-x}TiO_3$ and $Pb_xSr_{1-x}TiO_3$ are plotted in Figs. 7(b) and 7(c) for comparison. Similar anomalous line shape was also found in the $Pb_xBa_{1-x}TiO_3$ system. Contrary to Figs. 7(a) and 7(b), the asymmetric line shape of $A_1(1TO)$ mode of $Pb_xSr_{1-x}TiO_3$ (PST) in Fig. 7(c) was only observed in the region of $x \geqslant 0.9$, even though PST possesses the tetragonal phase in the region of $x > 0.5$. As previously mentioned, although PCT, PBT, and PST systems have similar perovskite structures, they exhibit diverse lattice dynamics. The observation of anharmonicity of $A_1(1TO)$ mode reflects directly the influence of various cation substitutions for Pb^{2+}. It has been well known that $SrTiO_3$ is quantum paraelectric; on the other hand, $BaTiO_3$ and $CaTiO_3$ show apparently successive transitions. Hidaka[41] has proposed that the necessary condition for displacive-type ferroelectrics is that the potential-energy profiles changes with temperature or pressure. In addition, it has also been concluded that the larger ζ parameter is the origin of the successive transitions. According to Hidaka's proposal,[41] PBT and PCT should have larger sixthorder potential term ζ than PST under the same A cation molar substitution for Pb^{2+}. Moreover, the tetragonal-to-cubic phase transition occurs at $x \sim 0.65$ and ~ 0.5 in PCT and PST systems, respectively. Under the same molar cation substitution for Pb^{2+}, the well depth of the potential should be larger in PST than in PCT but smaller than in PBT, which always possesses the tetragonal phase, to be in agreement with experimental results. Further, the absolute value of parameter ξ in PST should become smaller followed by Eq. (1), while more Sr content was added to lower the well depth of the potential enlarged by the smaller ζ compared with the other two systems. Based on the qualitative explication stated above, the anharmonicity nature may become negligible in the PST system because of the much smaller ζ and $|\xi|$ than those in the PCT and PBT systems as revealed in our experimental results.

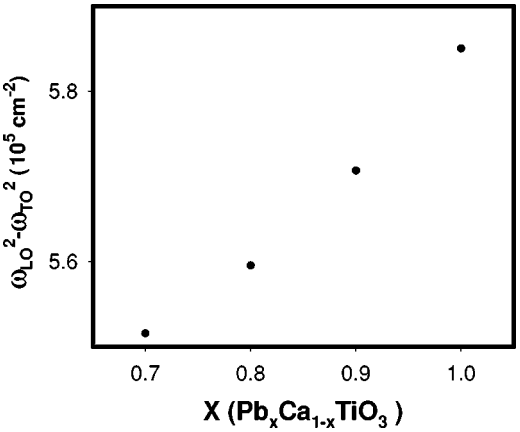

FIG. 8. Difference between square of A_1 (3LO) and $A_1(1TO)$ phonon frequencies for $Pb_xCa_{1-x}TiO_3$ in tetragonal phase.

Figure 8 shows another important observation associated with the lattice dynamics, which shows the difference between square of A_1 (3LO) and $A_1(1TO)$ phonon frequencies for $Pb_xCa_{1-x}TiO_3$ as $x > 0.7$. Obviously, the cell dimension of $Pb_xCa_{1-x}TiO_3$ decreases when x changes from 1 to 0.7 in Fig. 2. We expect that the shrinkage of lattice would lead to the giant LO-TO splitting while increase the Ca concentration. In clear contrast to the repulsion of giant LO-TO splitting in $Ba_xSr_{1-x}TiO_3$ system, however, Fig. 8 shows an attractive behavior similar to the $Pb_xSr_{1-x}TiO_3$ system by reducing tetragonality toward the cubic phase. Here, we conclude that the observed decreased LO-TO splitting for $PbTiO_3$-based compounds might be resulted from the contribution of $Z^*(A)$ to the mode effective charge due to the considerable hybridization of Pb-O bonding. Recently, our previous theoretical calculations and experimental spectra on O K-edge XANES (Ref. 37) have revealed that the partial substitution of A cation, Pb, by Ca not only decreases O $2p$-Pb $6p$ but also O $2p$-Ti $3d$ hybridization. Furthermore, the Ti $L_{3,2}$-edge measurements also find that the off-center displacement of Ti and ferroelectricity persist up to a Pb concentration between 0.6 and 0.7.[41] These results are consistent with our observations.

IV. CONCLUSION

In summary, the phase transitions of $Pb_xCa_{1-x}TiO_3$ samples prepared by sol-gel method have been investigated from XRD and Raman spectra. From the results of both XRD and Raman measurements, it indicates that there exist two obvious phase transitions. The first one occurring at $x \sim 0.65$ corresponds to the tetragonal-to-cubic phase. The second occurs near $x=0.35$ was attributed to the orthorhombic-to-cubic phase. Unlike the similar $Sr_xCa_{1-x}TiO_3$ system, no intermediate tetragonal phase was found between orthorhombic and cubic phases. The absence of the intermediate phase might be mostly attributed to the very restricted region in the PCT system. From the Raman results of $Pb_xCa_{1-x}TiO_3$, the consequences of the change of the broad $A_1(1TO)$ feature with decreasing x has been related to the softening and anharmonic effect. Moreover, diverse behavior of the anharmonicity of the $A_1(1TO)$ mode in PCT, PST, and PBT were observed. By comparing the line shape of $A_1(1TO)$ mode among PST, PBT, and PCT, we have concluded that the anharmonicity will become more conspicuous due to the larger ζ and $|\xi|$ in PCT and PBT systems. In addition, the phenomenon of LO-TO splitting similar to those found in PST system was investigated as well. The observed decreasing of LO-TO splitting as lower Pb concentration from 1 to 0.7 has been interpreted that the substitution of the A cation, Pb, by Ca not only decreases O $2p$-Pb $6p$ but also O $2p$-Ti $3d$ hybridization. We do hope the present study will encourage theoretical calculation to have further insight into lattice dynamics on ABO_3 perovskites.

ACKNOWLEDGMENTS

The work was supported by Grant No. NSC 92-2112-M009-037 from the National Science Council, Taiwan.

*Electronic address: wfhsieh@mail.nctu.edu.tw

[1] E. Cockayne and B.P. Burton, Phys. Rev. B **62**, 3735 (2000).
[2] R.D. King-Smith and D. Vanderbilt, Phys. Rev. B **49**, 5828 (1994).
[3] W. Zhong, R.D. King-Smith, and D. Vanderbilt, Phys. Rev. Lett. **72**, 3618 (1994).
[4] Ph. Ghosez, E. Cockayne, U.V. Waghmare, and K.M. Rabe, Phys. Rev. B **60**, 836 (1999).
[5] D. Vanderbilt and W. Zhong, Ferroelectrics **206**, 181 (1998).
[6] H.F. Kay and P.C. Bailey, Acta Crystallogr. **10**, 219 (1957).
[7] R. Ranjan and D. Pandey, J. Phys.: Condens. Matter **11**, 2247 (1999).
[8] R. Ranjan and D. Pandey, J. Phys.: Condens. Matter **13**, 4251 (2001).
[9] H.F. Naylor and O.A. Cook, J. Am. Chem. Soc. **68**, 1003 (1946).
[10] T. Vogt and W.W. Schmahl, Europhys. Lett. **24**, 281 (1993).
[11] S.A. Redfern, J. Phys.: Condens. Matter **8**, 8267 (1996).
[12] T. Matsui, H. Shigematsu, Y. Arita, Y. Hanajiri, N. Nakamitsu, and T. Nagasaki, J. Nucl. Mater. **247**, 72 (1997).
[13] B.J. Kennedy, C.J. Howard, and B.C. Chakoumakos, J. Phys.: Condens. Matter **11**, 1479 (1999).
[14] C.J. Ball, G.J. Thorogood, and E.R. Vance, J. Nucl. Mater. **190**, 298 (1992).
[15] X. Liu and R.C. Liebermann, Phys. Chem. Miner. **20**, 171 (1993).
[16] A.L. Kholkin, M.L. Calzada, P. Ramos, J. Mendiola, and N. Setter, Appl. Phys. Lett. **69**, 3602 (1996).
[17] A. Seifert, P. Muralt, and N. Setter, Appl. Phys. Lett. **72**, 2409 (1998).
[18] G. King, E. Goo, T. Yamamoto, and K. Okazaki, J. Am. Ceram. Soc. **71**, 454 (1988).
[19] G. King and E. Goo, J. Am. Ceram. Soc. **73**, 1534 (1990).
[20] R.E. Cohen, Nature (London) **358**, 136 (1992).
[21] S.Y. Kuo, C.T. Li, and W.F. Hsieh, Appl. Phys. Lett. **81**, 3019 (2002).
[22] C.M. Foster, Z. Li, M. Grimsditch, S.-K. Chan, and D.J. Lam, Phys. Rev. B **48**, 10 160 (1993).
[23] C.M. Foster, M. Grimsditch, Z. Li, and V.G. Karpov, Phys. Rev. Lett. **71**, 1258 (1993).
[24] J. Frantti, V. Lantto, S. Nishio, and M. Kakihana, Phys. Rev. B **59**, 12 (1999).
[25] J. Frantti and V. Lantto, Phys. Rev. B **54**, 12 139 (1996).
[26] S.Y. Kuo, W.Y. Liao, and W.F. Hsieh, Phys. Rev. B **64**, 224103 (2001).
[27] C.J. Ball, B.D. Begg, D.J. Cookson, G.J. Thorogood, and E.R. Vance, J. Solid State Chem. **139**, 238 (1998).
[28] R. Ranjan, D. Pandey, V. Siruguri, P.S.R. Krishna, and S.K. Paranjpe, J. Phys.: Condens. Matter **11**, 2233 (1999).
[29] S. Qin, A.I. Becerro, F. Seifert, J. Gottsmann, and J. Jiang, J. Mater. Chem. **10**, 1609 (2000).
[30] U. Balachandran and N.G. Eror, Solid State Commun. **44**, 815 (1982).
[31] T. Hirata, K. Ishioka, and M. Kitajima, J. Solid State Chem. **94**, 353 (1996).
[32] P. Gillet, F. Guyot, G.D. Price, B. Tournerie, and A.L. Cleach, Phys. Chem. Miner. **20**, 159 (1993).
[33] C.H. Perry, B.N. Khanna, and G. Rupprecht, Phys. Rev. **135**, A408 (1964).
[34] U. Balachandran and N.G. Eror, Solid State Commun. **44**, 815 (1982).
[35] P. McMillan and N. Ross, Phys. Chem. Miner. **16**, 21 (1988).
[36] P. Gillet, G. Fiquet, and I. Daniel, Geophys. Res. Lett. **20**, 1931 (1993).
[37] J.C. Jan, K. Kumar, J.W. Chiou, H.M. Tsai, H.L. Shih, H.C. Hsueh, S.C. Ray, K. Asokan, W.F. Pong, M.-H. Tsai, S.Y. Kuo, and W.F. Hsieh, Appl. Phys. Lett. **83**, 3311 (2003).
[38] A.F. Devonshire, Philos. Mag. **40**, 1040 (1949).
[39] S.M. Cho, H.M. Jang, and T.Y. Kim, Phys. Rev. B **64**, 014103 (2001).
[40] G.P. Srivastava, *The Physics of Phonons* (Adam Hilger, Bristol, 1990), Chap. 5.
[41] T. Hidaka, J. Phys. Soc. Jpn. **61**, 1054 (1992).